Stability of electrophoretic transport of ions

Prateek Gupta and Supreet Singh Bahga*

Department of Mechanical Engineering, Indian Institute of Technology Delhi, Hauz Khas, New Delhi 110016, India

(Received 31 March 2015; revised manuscript received 1 June 2015; published 10 August 2015)

We present an investigation of instability during electrophoretic transport of ions in a class of electrolytes called oscillating electrolytes. We analyze the onset of instability in electrophoretic transport in a binary electrolyte by modeling growth of small concentration disturbances over a base state with uniform acid and base concentrations. Our linear stability analysis shows that the growth rate of low wave-number concentration disturbances increases with an increase in wave number. Whereas, the growth rate of high wave-number disturbances decreases with increasing wave number due to the stabilizing effect of molecular diffusion. Our analysis also yields the scaling for growth rates and the wave number of most unstable mode with electric field. In addition, we show that the electrophoretic system exhibits instability only for a certain range of species concentrations. We also discuss the physical mechanism underlying the instability of transport process. We show that the instability is exhibited by those binary electrolytes that consist of a multivalent species with unusually high electrophoretic mobility in higher ionization states. Throughout, we provide verification of our linear stability analysis with full nonlinear simulations.

DOI: 10.1103/PhysRevE.92.022301 PACS number(s): 82.45.−h

I. INTRODUCTION

The motion of ions in an electrolyte solution induced by an applied electric field is termed electrophoretic transport. Electrophoretic transport is widely employed in analytical chemistry techniques such as capillary zone electrophoresis (CZE) [1], isotachophoresis (ITP) [2], and field amplified sample stacking (FASS) [3], wherein differential electromigration velocities of ions are used for separation and in some cases preconcentration of ionic species from sample mixtures. Typical electrophoresis experiments are performed in microcapillaries having diameter of $\mathcal{O}(10\text{–}100\,\mu\text{m})$, in which electric field of $\mathcal{O}(10\text{kV/m})$ leads to electrophoretic motion of ions having velocity of $\mathcal{O}(1\text{ mm/s})$.

The differential electrophoretic velocities of ions lead to a variety of propagating waves in ion concentrations, which are essentially propagating disturbances in the concentration field. Depending upon the initial conditions, both linear and nonlinear waves are observed in electrophoresis. For example, CZE is characterized by propagation of linear waves corresponding to sample zones migrating under axially uniform electric field [4]. Whereas nonlinear waves are observed in electrophoretic techniques such as ITP, wherein coupling of ion concentrations with local electric field (due to the Ohm's law) result in propagating shock waves [5]. Analogous to waves in other physical processes, such as in compressible flow and shallow water flow, waves in electrophoresis are a consequence of finite propagation speed of concentration disturbances. In other words, the transport equations that govern the motion of ions have a flux vector whose Jacobian matrix has real-valued eigenvalues; these eigenvalues are often referred to as eigenmobilities while describing electrophoretic phenomenon [4,6].

Previously, electrophoretic transport phenomenon was thought to exhibit only wave propagation phenomena. However, recently Hruska *et al.* [7] discovered a binary electrolyte system consisting of sebacic acid and imidazole that becomes unstable under the influence of electric field. Through a series of experiments, Hruska *et al.* demonstrated that for particular concentrations of sebacic acid and imidazole, small perturbations in initially uniform concentration field amplify over time under applied electric field and result in propagating, oscillatory modes in ion concentrations. In addition, Hruska *et al.* used the linear electromigration theory [8] to show that such electrophoretic transport of ions is characterized by complex valued eigenmobilities, due to which the effect of local perturbations in concentration are felt elsewhere instantaneously. The analysis of Hruska *et al.* was limited to a unique binary electrolyte system (sebacic acid and imidazole). Subsequently, Riesova *et al.* [9] experimentally demonstrated a wider class of ternary electrolytes, which exhibit similar unstable behavior.

Existing analyses of instabilities in electrophoretic transport are based on the linear electromigration theory [8], in which electromigration flux of ionic species is linearized over a base state to model spatiotemporal evolution of perturbations in concentration field. Such analyses are able to distinguish between electrolytes, which exhibit stable and unstable electrophoretic motion of ions. However, since the effect of molecular diffusion and diffusive current are not accounted for in the existing models, these models wrongly predict the growth rates of disturbances in species concentrations. For example, existing models predict that the growth rate of instability increases linearly with the wave number of concentration perturbation; therefore, all modes are predicted to be unstable. However, experiments show unstable modes with intermediate wave numbers due to their higher growth rates compared with low and high wave-number modes. This is because, at high wave numbers (corresponding to steeper gradients) diffusion is more pronounced, which renders the system stable to concentration disturbances. Moreover, the existing framework for analyzing unstable electrophoretic transport does not explain the effect of electric field on the wave number of unstable modes.

*bahga@mech.iitd.ac.in

In this paper, we present linear stability analysis of electrophoretic transport in a binary electrolyte consisting of sebacic acid and imidazole. Our analysis is based on a detailed, three-dimensional (3D), nonlinear mathematical model of electrophoretic transport, which includes the effects of electromigration, molecular diffusion, diffusive current, and acid-base equilibria. Based on the linear stability analysis we obtain the conditions for marginal stability. In particular, we show the effect of applied electric field, electrolyte composition, and perturbation wave numbers on the stability of electrophoretic transport. Our analysis captures the competing effects of electromigration and diffusion, and hence provides the wave number with maximum growth rate. In addition, we provide the scaling of growth rates and the most unstable wave number with electric field. We have verified the results from linear stability analysis, including those for scaling with electric field, with simulations of nonlinear species transport equations. Although the results we present here are for a specific binary electrolyte system, our approach and general conclusions are valid even for multispecies electrolyte systems. Before concluding, we elucidate the physical mechanism underlying the onset of instabilities during electrophoretic transport of ions.

II. MATHEMATICAL MODEL

The transport equations that govern the spatiotemporal evolution of ionic species migrating under the influence of electric field $\mathbf{E}$ in absence of bulk fluid motion are given by [10]

$$\frac{\partial c_i}{\partial t} + \nabla \cdot (\mu_i c_i \mathbf{E}) = \nabla^2 (D_i c_i), \quad i = 1 \ldots, N, \tag{1}$$

where c_i, μ_i, and D_i, respectively, denote the total (analytical) concentration, the effective electrophoretic mobility, and the effective diffusivity of species family i. The term "species family" refers to all ionization states of a species such that $i =$ sebacic acid has three ionization states, $z = -2, -1$, and 0, and $i =$ imidazole has two ionization states, $z = 1$ and 0. The total concentration c_i is related to the concentrations of various ionization states $c_{i,z}$ of species family i by $c_i = \sum_z c_{i,z}$. The effective mobility and effective diffusivity are defined as weighted average of mobilities and diffusivities of various ionization states ($\mu_{i,z}$ and $D_{i,z}$) with ionization fractions $g_{i,z}$ as the weights,

$$\mu_i = \sum_z \mu_{i,z} g_{i,z}, \quad D_i = \sum_z D_{i,z} g_{i,z}, \quad g_{i,z} = \frac{c_{i,z}}{c_i}. \tag{2}$$

The ionization fractions can be obtained by assuming local chemical equilibrium between different chemical species (see Sec. II A). The assumption of local chemical equilibrium is justified because the timescale associated with acid-base dissociation reactions is significantly smaller than the timescales for electromigration and molecular diffusion [10].

Next, by assuming local electroneutrality and invoking continuity of current (Ohmic and diffusion currents), electric field can be related with species concentrations as

$$\nabla \cdot (\sigma \mathbf{E} - \nabla S) = 0. \tag{3}$$

Here σ and ∇S denote the electrical conductivity and the diffusion current, respectively. In terms of ionic concentrations, the electrical conductivity and diffusion current are given by

$$\sigma = \sum_i \sum_z z_{i,z} \mu_{i,z} c_{i,z} F + \mu_H c_H F - \mu_{OH} c_{OH} F, \tag{4}$$

$$\nabla S = F \nabla \left(\sum_i \sum_z z_{i,z} D_{i,z} c_{i,z} + D_H c_H - D_{OH} c_{OH} \right), \tag{5}$$

where F is the Faraday's constant and subscripts H and OH denote hydronium and hydroxyl ions, respectively.

A. Binary electrolyte

In order to solve the transport equations Eq. (1), it is necessary to calculate the ionization fractions, which determine the effective mobility and diffusivity of a species family. Here we limit our discussion to a general binary electrolyte system consisting of a divalent acid H_2A (e.g., sebacic acid) and a univalent base BOH (e.g., imidazole) and calculate the ionization fractions for acid and base. The acid-base dissociation reactions of this electrolyte system are given by

$$H_2A \rightleftharpoons H^+ + HA^- \quad K_{A,-1} = \frac{c_{A,-1} c_H}{c_{A,0}}, \tag{6}$$

$$HA^- \rightleftharpoons H^+ + A^{-2} \quad K_{A,-2} = \frac{c_{A,-2} c_H}{c_{A,-1}}, \tag{7}$$

$$B^+ + H_2O \rightleftharpoons BOH + H^+ \quad K_{B,1} = \frac{c_{B,0} c_H}{c_{B,1}}, \tag{8}$$

where K is the corresponding equilibrium constant. Using Eqs. (6) and (7), the fraction of acid in various ionization states $g_{A,z} = c_{A,z}/c_A$ can be expressed as functions of hydronium ion concentration c_H as

$$g_{A,0} = \frac{c_H^2}{d_A}, \; g_{A,-1} = \frac{K_{A,-1} c_H}{d_A}, \; g_{A,-2} = \frac{K_{A,-1} K_{A,-2}}{d_A}, \tag{9}$$

where $d_A = c_H^2 + K_{A,-1} c_H + K_{A,-1} K_{A,-2}$. Similarly, using Eq. (8) ionization fractions for the base $g_{B,z} = c_{B,z}/c_B$ can be related with c_H as

$$g_{B,0} = \frac{K_{B,1}}{K_{B,1} + c_H}, \quad g_{B,1} = \frac{c_H}{K_{B,1} + c_H}. \tag{10}$$

Finally, knowing the total concentrations of acid and base, the concentration of hydronium ion can be calculated using the electroneutrality assumption,

$$-c_{A,-1} - 2c_{A,-2} + c_{B,1} + c_H - \frac{K_w}{c_H} = 0, \tag{11}$$

where $K_w = c_H c_{OH}$ is the ionization constant of water.

Given the total concentrations of acid and base, the concentrations of acid and base in various ionization states can be obtained by solving Eqs. (9), (10), and (11). Knowing the concentrations of acid and base in various ionization states, the species transport equations Eq. (1) can be rewritten

as

$$\frac{\partial c_A}{\partial t} + \nabla \cdot [(\mu_{A,-1}c_{A,-1} + \mu_{A,-2}c_{A,-2})\mathbf{E}] = \nabla \cdot (D_{A,0}\nabla c_{A,0} + D_{A,-1}\nabla c_{A,-1} + D_{A,-2}\nabla c_{A,-2}), \tag{12}$$

$$\frac{\partial c_B}{\partial t} + \nabla \cdot (\mu_{B,1}c_{B,1}\mathbf{E}) = \nabla \cdot (D_{B,0}\nabla c_{B,0} + D_{B,1}\nabla c_{B,1}). \tag{13}$$

The local electric field is governed by Eq. (3), where conductivity σ and diffusion current ∇S are given by

$$\sigma = F\Big(-\mu_{A,-1}c_{A,-1} - 2\mu_{A,-2}c_{A,-2} + \mu_{B,1}c_{B,1} + \mu_H c_H - \mu_{OH}\frac{K_w}{c_H}\Big), \tag{14}$$

$$\nabla S = F\nabla\Big(-D_{A,-1}c_{A,-1} - 2D_{A,-2}c_{A,-2} + D_{B,1}c_{B,1} + D_H c_H - D_{OH}\frac{K_w}{c_H}\Big), \tag{15}$$

respectively.

B. Linear stability analysis

Here we analyze the stability of electrophoretic transport of ions when electric field is applied through a binary electrolyte composed of a divalent acid and a monovalent base. The electrolyte is filled in a cylindrical capillary of diameter d and electric field $E_0\hat{\mathbf{x}}$ is applied externally along the axis of capillary (x direction) as shown schematically in Fig. 1. We assume that the inner wall of capillary is uncharged, and hence there is no electroosmotic flow. This assumption has no effect on overall conclusions regarding concentration instabilities since the bulk fluid only affects the translation of concentration disturbances. Since the electric field is tangential at the surface of inner wall, the no-flux boundary condition at the wall simplifies to

$$\frac{\partial c_A}{\partial r} = \frac{\partial c_B}{\partial r} = 0 \quad \text{at} \quad r = \frac{d}{2}. \tag{16}$$

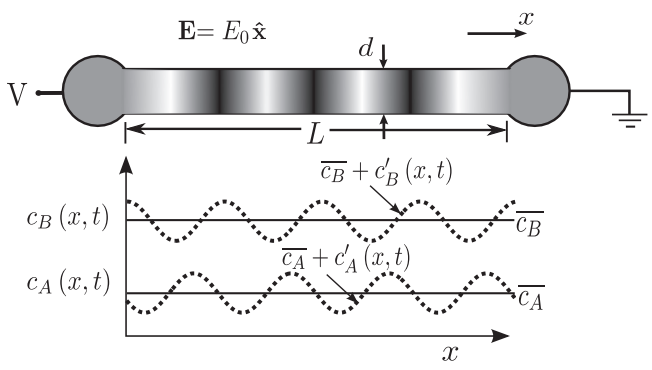

FIG. 1. Schematic illustrating the base state and the perturbed state of an unstable electrophoretic system consisting of a binary electrolyte. Initially, the channel is filled uniformly with binary electrolyte consisting of sebacic acid (H_2A) and imidazole (BOH). When electric field $\mathbf{E}$ is applied along the axial direction, the electrophoretic motion of ions induced in the capillary becomes unstable and small perturbations in concentration field grow over time.

In the base state, the species concentrations and the local electric field are spatially uniform:

$$c_A(x,r,\theta,t) = \bar{c}_A, \quad c_B(x,r,\theta,t) = \bar{c}_B, \quad c_H(x,r,\theta,t) = \bar{c}_H, \quad \mathbf{E}(x,r,\theta,t) = E_0\hat{\mathbf{x}}. \tag{17}$$

Here overbars denote the base-state variables. To perform linear stability analysis we introduce the following perturbation variables:

$$c_A = \bar{c}_A + c'_A(x,r,\theta,t), \quad c_B = \bar{c}_B + c'_B(x,r,\theta,t), \quad c_H = \bar{c}_H + c'_H(x,r,\theta,t), \quad \mathbf{E} = E_0\hat{\mathbf{x}} + \mathbf{E}'(x,r,\theta,t), \tag{18}$$

where primes denote the perturbation variables. Substituting the perturbation variables in the governing equations, Eqs. (3), (12), and (13), and linearizing the resulting equations yields

$$\frac{\partial c'_A}{\partial t} + \bar{\mu}_A\bar{c}_A\nabla\cdot\mathbf{E}' + E_0\frac{\partial}{\partial x}(\mu_{A,-1}c'_{A,-1} + \mu_{A,-2}c'_{A,-2}) = \nabla\cdot(D_{A,0}\nabla c'_{A,0} + D_{A,-1}\nabla c'_{A,-1} + D_{A,-2}\nabla c'_{A,-2}), \tag{19}$$

$$\frac{\partial c'_B}{\partial t} + \bar{\mu}_B\bar{c}_B\nabla\cdot\mathbf{E}' + E_0\frac{\partial}{\partial x}(\mu_{B,1}c'_{B,1}) = \nabla\cdot(D_{B,0}\nabla c'_{B,0} + D_{B,1}\nabla c'_{B,1}), \tag{20}$$

$$\bar{\sigma}\nabla\cdot\mathbf{E}' + E_0\frac{\partial\sigma'}{\partial x} - \nabla^2 S' = 0. \tag{21}$$

The perturbation conductivity, σ', and diffusion current $\nabla S'$ depend on other perturbation variables as

$$\sigma' = F\Big(-\mu_{A,-1}c'_{A,-1} - 2\mu_{A,-2}c'_{A,-2} + \mu_{B,1}c'_{B,1} + \mu_H c'_H + \mu_{OH}\frac{K_w c'_H}{\bar{c}_H^2}\Big), \tag{22}$$

and

$$\nabla S' = F\nabla\Big(-D_{A,-1}c'_{A,-1} - 2D_{A,-2}c'_{A,-2} + D_{B,1}c'_{B,1} + D_H c'_H + D_{OH}\frac{K_w c'_H}{\bar{c}_H^2}\Big). \tag{23}$$

The perturbation concentrations of various ionization states of acid and base can be related to perturbations in total concentrations and hydronium ion concentration by linearizing $c_{i,z} = c_i g_{i,z}$ over the base state. That is,

$$c'_{i,z} = c'_i\bar{g}_{i,z} + \bar{c}_i\frac{\partial g_{i,z}}{\partial c_H}\Big|_{c_H=\bar{c}_H}c'_H, \quad i = A,B. \tag{24}$$

The perturbation hydronium ion concentration is obtained using the electroneutrality assumption Eq. (11),

$$-c'_{A,-1} - 2c'_{A,-2} + c'_{B,1} + c'_H + \frac{K_w}{\bar{c}_H^2}c'_H = 0, \tag{25}$$

Finally, eliminating $\nabla \cdot \mathbf{E}'$, $c'_{i,z}$, and c'_H from Eqs. (19) and (20) and using Eqs. (21), (24), and (25) we obtain a set of linearized transport equations in terms of perturbation concentrations of the acid and the base:

$$\frac{\partial}{\partial t}\begin{pmatrix} c'_A \\ c'_B \end{pmatrix} + \mathbf{M}E_0 \frac{\partial}{\partial x}\begin{pmatrix} c'_A \\ c'_B \end{pmatrix} = \mathbf{D}\nabla^2 \begin{pmatrix} c'_A \\ c'_B \end{pmatrix}. \tag{26}$$

Here $\mathbf{M}$ and $\mathbf{D}$ are matrices having units of mobility and diffusivity, respectively. Detailed derivation of Eq. (26) and expressions for $\mathbf{M}$ and $\mathbf{D}$ are provided in the Appendix. Since the base-state concentration field is spatially uniform, the boundary conditions Eq. (16) can be expressed in terms of perturbation concentrations as

$$\frac{\partial c'_A}{\partial r} = \frac{\partial c'_B}{\partial r} = 0 \quad \text{at} \quad r = \frac{d}{2}. \tag{27}$$

C. Normal modes analysis

We here analyze the stability of electrophoretic transport of ions due to disturbances in the concentration field. An arbitrary perturbation in concentration field can be assumed to be a linear combination of various oscillatory modes. Since the governing equations Eq. (26) and the boundary conditions Eq. (27) are linear, stability of the electrophoretic system to an arbitrary disturbance can be analyzed by considering stability of individual perturbation modes. Therefore, we assume the solution for the perturbation concentrations of the form

$$\begin{pmatrix} c'_A(x,r,\theta,t) \\ c'_B(x,r,\theta,t) \end{pmatrix} = \begin{pmatrix} \tilde{c}'_A(r) \\ \tilde{c}'_B(r) \end{pmatrix} e^{ikx+in\theta+st}. \tag{28}$$

Substituting this form of solution in the linearized equations Eq. (26) and boundary conditions Eq. (27) we obtain the following set of coupled ordinary differential equations,

$$\mathbf{D}\left(\frac{1}{r}\frac{d}{dr}r\frac{d}{dr} - k^2 - \frac{n^2}{r^2}\right)\begin{pmatrix} \tilde{c}'_A \\ \tilde{c}'_B \end{pmatrix} = (ik\mathbf{M}E_0 + s\mathbf{I})\begin{pmatrix} \tilde{c}'_A \\ \tilde{c}'_B \end{pmatrix}, \tag{29}$$

and boundary conditions,

$$\frac{d\tilde{c}'_A}{dr} = \frac{d\tilde{c}'_B}{dr} = 0 \quad \text{at} \quad r = \frac{d}{2}. \tag{30}$$

Equation (29) and the boundary conditions Eq. (30) suggest a solution of the form

$$\tilde{c}'_A(r) = A_n J_n(|p|r), \quad \tilde{c}'_B(r) = B_n J_n(|p|r), \tag{31}$$

where $n = 0,1,2,\ldots$. Here J_n denotes the Bessel's function of the first kind and $|p|$ are the roots of the equation $J'_n(|p|d/2) = 0$ so as to satisfy the boundary conditions given by Eq. (30). Substituting the solutions for $\tilde{c}'_A$ and $\tilde{c}'_B$, Eq. (31) in the linearized governing equations Eq. (29) we obtain a matrix eigenvalue problem for the growth rate s for various n and wave numbers k,

$$[ik\mathbf{M}E_0 + (k^2 + p^2)\mathbf{D} + s\mathbf{I}]\begin{pmatrix} A_n \\ B_n \end{pmatrix} = 0. \tag{32}$$

Equation (32) suggests that the diffusive effects in the electrophoretic system are more pronounced for nonzero values of p. Since diffusion has a stabilizing effect on the electrophoretic transport, the maximum growth rate occurs for $p = 0$. That is, the eigenmodes corresponding to $p = 0$ are expected to be dominant during the instability. Therefore, unless otherwise specified, we use $p = 0$ for all our calculations. In addition to the results for $p = 0$, later in Fig. 3 and the related discussion in Sec. III A, we present the growth rates for nonzero values of p to show that the eigenmodes corresponding to $p = 0$ have the largest growth rate.

For $p = 0$, nontrivial solutions satisfying Eq. (30) exist only for $n = 0$, which suggests that axisymmetric modes are most unstable. The growth rates for the axisymmetric perturbations are given by

$$\det(i\hat{k}\mathbf{M} + \hat{k}^2\mathbf{D} + \hat{s}\mathbf{I}) = 0, \tag{33}$$

where $\hat{k} = k/E_0$ and $\hat{s} = s/E_0^2$ are the scaled perturbation wave number and growth rate, respectively. In general, growth rate s given by Eq. (32) is complex-valued, $s = s_R + is_I$. Most electrophoretic systems consisting of a divalent acid and a univalent base have growth rate s with negative real part ($s_R < 0$). In such systems, the electrophoretic transport does not exhibit oscillatory behavior as concentration disturbances diminish over time. However, certain binary electrolytes, such as the mixture of sebacic acid and imidazole, can have growth rates s with positive real part ($s_R > 0$), depending upon the concentrations of acid and base. In such systems, small disturbances in species concentrations amplify over time, resulting in oscillatory modes that propagate at a speed of s_I/k. In Sec. III A we show that for unstable electrophoretic transport of ions the growth rate is maximum for a particular axisymmetric mode. Moreover, the scaling $\hat{k} = k/E_0$ and $\hat{s} = s/E_0^2$ suggests that the wave number of most unstable mode scales as E_0, while the corresponding growth rate scales as E_0^2.

III. RESULTS AND DISCUSSIONS

In this section, we discuss the effects of electric field, wave number of concentration disturbances, and species concentrations on the stability of electrophoretic transport. For all our calculations, we consider a binary electrolyte consisting of sebacic acid ($\mu_{A,-1} = -20.7 \times 10^{-9}\ \mathrm{m^2V^{-1}s^{-1}}$, $\mathrm{p}K_{A,-1} = 4.53$; $\mu_{A,-2} = -44.9 \times 10^{-9}\ \mathrm{m^2V^{-1}s^{-1}}$, $\mathrm{p}K_{A,-2} = 5.38$) and imidazole ($\mu_{B,1} = 52.0 \times 10^{-9}\ \mathrm{m^2V^{-1}s^{-1}}$, $\mathrm{p}K_{B,1} = 7.15$). The values of molecular diffusivity of charged species were calculated using the Stokes-Einstein relation, $D_{i,z} = \mu_{i,z}RT/zF$, where R is the universal gas constant and $T = 298$ K is the temperature of electrophoretic system. The diffusivity of neutral species was taken to be the mean value of diffusivities of the corresponding charged species. We also verify the results obtained from our linearized model with nonlinear simulations. For full nonlinear numerical simulations we use experimentally validated nonlinear numerical solver for electrophoresis, SPRESSO [11]. Last, we discuss the physical mechanism underlying the instability during electrophoretic transport.

A. Instability growth rates

We calculated the growth rates for most unstable mode with $p = 0$ using Eq. (32) for varying wave numbers and electric fields. The electrolyte that we consider here is composed of 0.21 mM sebacic acid and 0.323 mM imidazole. In addition, to verify the growth rates predicted by the linearized model we performed simulations using nonlinear species transport

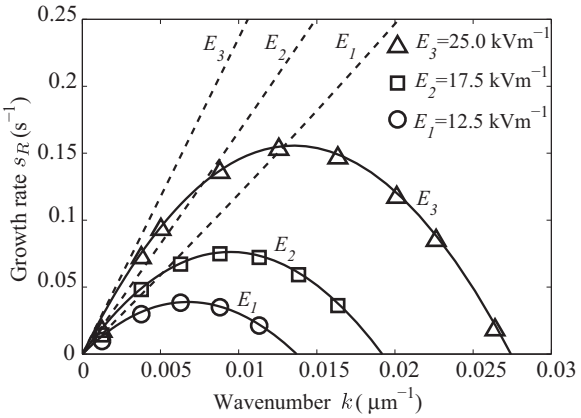

FIG. 2. Growth rates for most unstable mode with $p = 0$ for varying electric field and wave number. Data points show the growth rates predicted by nonlinear simulations. Solid lines show the growth rates predicted by the current model. Dashed lines show the growth rates predicted by the linear electromigration theory where diffusion is neglected. When diffusive effects are neglected (dashed lines) the growth rates increase linearly with perturbation wave numbers, indicating that all perturbation modes are unstable. However, when diffusive effects are accounted for (solid lines) the growth rates decrease at high wave numbers as diffusion is prominent when concentration gradients are large. These calculations are for a binary electrolyte system composed of 0.21 mM sebacic acid and 0.323 mM imidazole.

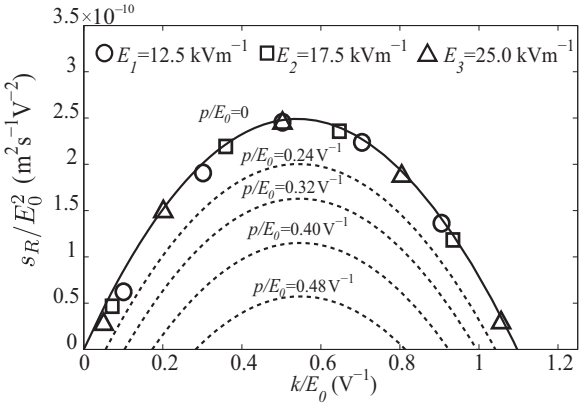

FIG. 3. Comparison of growth rates predicted by linearized model and nonlinear simulations. Data points (nonlinear simulations) and solid lines (linearized model) show results presented in Fig. 2 for axisymmetric perturbation modes ($p = 0$) plotted using the scaled growth rate s_R/E_0^2 and wave number k/E_0. The growth rates for different electric fields collapse on a single curve corresponding to $p = 0$. The dashed lines correspond to the growth rates for nonaxisymmetric perturbation modes ($p \neq 0$). Due to higher diffusive effects at $p \neq 0$, the growth rates are lower compared with those of axisymmetric perturbation modes with $p = 0$.

equations Eqs. (12)–(15). For the nonlinear simulations, we used initial conditions with concentration perturbations of a particular wave number over the base state. We extracted the growth rates from the simulation results by least-squares fitting of exponential curves to the variation of perturbation amplitude with time. For all these calculations, the concentration perturbations were at least six orders of magnitude smaller than the base-state concentrations so as to ensure linear system response.

Figure 2 shows the variation of real part of growth rate s with wave number of perturbation k predicted by the linearized model (solid lines) and nonlinear simulations (data points). The results show that the electrophoretic system is unstable over a particular range of wave numbers. For perturbation modes with smaller wave numbers, the growth rate of instability increases with the wave number. However, for perturbations with large wave numbers where stabilizing effect of diffusion is prominent, the growth rate decreases with wave number and eventually becomes negative. The results presented in Fig. 2 also show that the growth rates predicted by the linearized model compare well with those predicted by experimentally validated nonlinear numerical solver [11].

To highlight the stabilizing effect of diffusive flux, in Fig. 2 we also plot the growth rates predicted by the linearized model of Hruska *et al.* [7] (dashed lines), wherein molecular diffusion is not accounted for. The results show that the growth rates are grossly overpredicted when diffusion is neglected. Moreover, in absence of diffusion, the growth rates increase linearly with wave number. Thus, we conclude that the stabilizing effect of diffusion counteracts the destabilizing effect of electromigration causing the growth rate to attain a maxima at an intermediate wave number. The perturbation mode corresponding to the largest growth rate can be expected to be observed during the initial phase of instability, when the conditions for linear approximation prevail.

Figure 2 also shows that the applied electric field has a significant effect on the range of wave numbers of unstable modes and their growth rates. To quantify the effect of electric field on instability growth rates, in Fig. 3 we plot all the data shown in Fig. 2 by using the scaled values of growth rate s_R/E_0^2 and wave number of perturbation k/E_0. As predicted by Eq. (33), the growth rates computed using the linear and nonlinear models collapse on a single curve. Therefore, the theoretical scaling for wave numbers and their respective growth rates allows us to characterize an unstable electrophoretic system for varying electric fields. The theoretical scaling shows that increase in electric field increases the range of unstable wave numbers and their growth rates. Moreover, the wave number of most unstable mode increases proportionally with electric field.

The growth rates presented in Fig. 2 and the corresponding scaled growth rates depicted by the solid line in Fig. 3 are for the most unstable mode with $p = n = 0$; this mode is axisymmetric. As discussed in Sec. II C the nonaxisymmetric modes (with $p \neq 0$) have lower growth rates. To illustrate this, we present the growth rates for nonaxisymmetric modes with $p \neq 0$ in Fig. 3 (dashed lines). Compared with the axisymmetric modes, the nonaxisymmetric modes have lower growth rates for all wave numbers and values of p. Note that the results presented here for nonzero values of p hold for all n such that the boundary conditions given by Eq. (30) are satisfied, that is, $J_n'(|p|d/2) = 0$.

B. Effect of species concentration

Next, we discuss the effect of base state species concentrations on the electrophoretic transport instability exhibited by sebacic acid and imidazole mixture. Hruska *et al.* [7] noted

that electrophoretic transport of ions in this electrolyte mixture exhibits unstable behavior only in a certain range of acid and base concentrations. Their analysis was based on finding the electrolyte composition at which the mobility matrix **M** (Jacobian of electromigration flux vector) has complex valued eigenvalues. The diffusion-free model of Hruska *et al.* correctly identifies the concentration range of acid and base over which the electrophoretic system becomes unstable. However, as noted in the previous section, the growth rates are wrongly predicted by the linearized model when diffusion is neglected.

We computed the growth rates of perturbation modes for varying species concentrations using Eq. (33), which takes into account the competing effects of electromigration and diffusion. For our calculations, we fixed the base-state concentration of sebacic acid at 0.21 mM and varied the base state concentration of imidazole. Figure 4 shows the variation of growth rates for varying concentration of imidazole. The results show that variation in imidazole concentration affects the growth rate and the wave-number range of unstable modes. Also, for a fixed concentration of sebacic acid (0.21 mM), there exists a critical concentration of imidazole at which the system has higher values of growth rate and larger wave-number range of unstable perturbation modes, making it more susceptible to the instability.

An alternate way of illustrating the effect of concentrations of acid and base on the stability of electrophoretic transport is through neutral stability curves. In Fig. 5(a) we plot the neutral stability curves showing concentration of imidazole versus

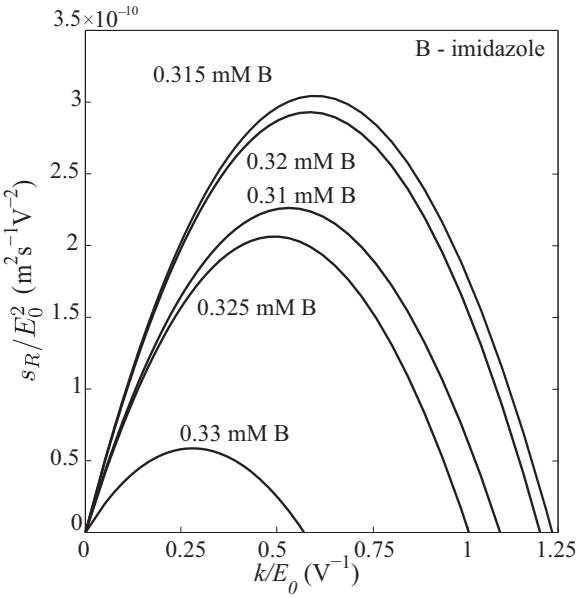

FIG. 4. Effect of base-state electrolyte composition on instability growth rates. Shown here are growth rates versus wave number for base state with 0.21 mM sebacic acid and varying concentrations of imidazole. For relatively low and high imidazole concentrations, the electrophoretic transport is unstable for small wave-number range of perturbation modes and these modes have small growth rates. However, for intermediate imidazole concentrations, the electrophoretic system is more susceptible to instability due to larger wave-number range of unstable perturbation modes and higher growth rates.

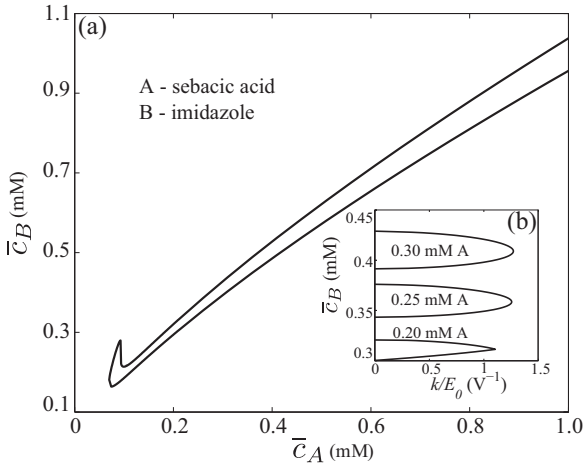

FIG. 5. Effect of base-state electrolyte composition on the stability of electrophoretic transport of ions. (a) Neutral stability curves for electrolyte consisting of sebacic acid and imidazole. The region enclosed by the curve corresponds to the base states for which electrophoretic system is unstable. (b) Neutral stability curves for varying base-state composition and wave numbers scaled by electric field. The region enclosed within the curves corresponds to unstable regime. The wave-number range of unstable perturbation modes varies with the base-state composition.

concentration of sebacic acid for which the most unstable mode is neutrally stable. The region enclosed within the neutral stability curve corresponds to the unstable regime. Whereas, the region outside the neutral stability curves corresponds to conditions at which none of the perturbation modes in species concentrations grow. In other words, the neutral stability diagram separates the concentration regime at which perturbations with all wave numbers are stable from those where at least some perturbation modes are unstable. The neutral stability curve in Fig. 5(a) suggests that for unstable electrophoretic transport of ions the perturbations grow until they attain local concentrations, which lie on the neutral stability curve. We note that, for the unstable concentration regime enclosed by the neutral stability curve in Fig. 5(a), perturbations with only certain wave numbers are unstable. The range of the wave numbers of these unstable modes depends on the base-state composition, as shown in Fig. 5(b). Here, the region enclosed within the curves corresponds to the conditions at which the system is unstable.

C. Physics of unstable electrophoretic transport

In this section, we elucidate the physical mechanism underlying instability of electrophoretic transport of ions. We limit our discussion to a generalized binary electrolyte system consisting of a divalent acid and a univalent base. Here we neglect the effect of diffusion and focus on the effect of perturbations in concentration field on electromigration flux. This is because electromigration is solely responsible for instability and the only role of diffusion is to stabilize the system by reducing the gradients in species concentrations.

When the conditions for unstable electrophoretic transport prevail, small perturbations in concentration field alter the electromigration flux in a way that the perturbations are further

amplified. To demonstrate this, we consider spatiotemporal evolution of acid concentration due to perturbation in concentrations of acid and base. The concentration of acid c_A (ignoring molecular diffusion) is governed by

$$\frac{\partial c_A}{\partial t} + \frac{\partial f_A}{\partial x} = 0, \quad f_A = \mu_A c_A \frac{j}{\sigma}, \tag{34}$$

where f_A denotes the electromigration flux. In Eq. (34) we have ignored diffusive current and used the Ohm's law to relate local electric field E with current density j and conductivity σ. The effective mobility μ_A and conductivity σ are given by

$$\mu_A = \mu_{A,-1}\frac{c_{A,-1}}{c_A} + \mu_{A,-2}\frac{c_{A,-2}}{c_A}, \tag{35}$$

and

$$\sigma = F\Big(-\mu_{A,-1}c_{A,-1} - 2\mu_{A,-2}c_{A,-2} + \mu_{B,1}c_{B,1} + \mu_H c_H - \mu_{OH}\frac{K_w}{c_H}\Big), \tag{36}$$

respectively.

Next, we consider a particular mode of concentration perturbation shown in Fig. 6. To illustrate the destabilizing effect of electromigration flux, we consider two axial locations x_1 and x_2 lying on the opposite sides of local maxima in acid concentration. The local concentration of acid is the same at x_1 and x_2. For the perturbation mode shown in Fig. 6, the concentration of base is higher at x_2 than at x_1. Therefore, the local pH at x_2 is higher than that at x_1. Consequently, the equilibrium composition of the acid at x_2 shifts toward the higher ionization state compared with that at x_1. In other words, compared with x_1, $c_{A,-1}$ is lower and $c_{A,-2}$ is higher at x_2. Since $|\mu_{A,-2}| > |\mu_{A,-1}|$, increase in $c_{A,-2}$ and decrease in $c_{A,-1}$ results in an increase in the magnitude of effective

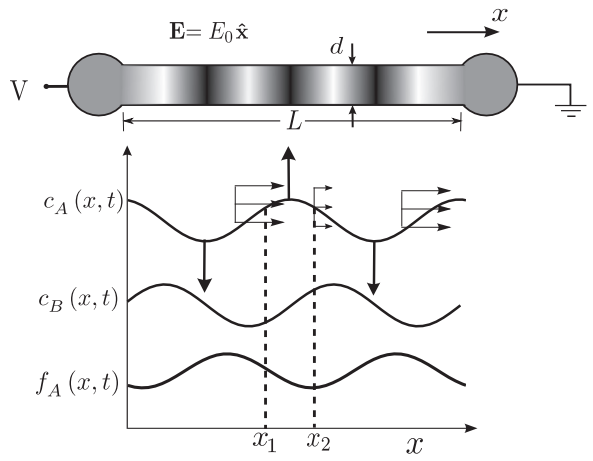

FIG. 6. Schematic illustrating the destabilizing effect of electrophoretic flux due to concentration perturbations. The transport of ions as a result of arbitrary perturbations can be studied as a linear combination of harmonic modes. Shown here is a perturbation mode, which changes the electromigration flux in a way that the flux is higher at location x_1 and lower at x_2. As a result, the local maxima and minima in acid concentration increases and decreases, respectively, leading to instability.

mobility μ_A of acid and conductivity σ [from Eqs. (35) and (36)]. In a majority of binary electrolyte systems, such an increase in effective mobility and the corresponding increase in conductivity offset each other resulting in no change in the electromigration flux given by Eq. (34). However, for electrolytes consisting of acidic species with unusually high value of $\mu_{A,-2}/\mu_{A,-1}$ (e.g., $\mu_{A,-2}/\mu_{A,-1} = 2.2$ for sebacic acid) the relative change in conductivity due to the change in pH is higher than that in effective mobility. For such electrolytes, the magnitude of electromigration flux, which is given by Eq. (34), is lower at x_2 than at x_1. Consequently, the mass of acid accumulates between locations x_1 and x_2 and the acid concentration increases at the location of maxima as shown in Fig. 6. Similarly, the minimum concentration of acid decreases. Analogously, it can be shown that the abnormal increase in conductivity due to high $\mu_{A,-2}/\mu_{A,-1}$ ratio causes local maxima and minima in the concentration of base to increase and decrease, respectively. As a result, small disturbances in the concentration field amplify over time resulting in observable oscillations in species concentrations.

To confirm the mechanism of instability we studied the evolution of perturbation modes using full nonlinear simulations. For our simulations, we considered base-state electrolyte composition of 0.21 mM sebacic acid and 0.323 mM imidazole. We perturbed the uniform quiescent base state with in-phase perturbations in acid and base concentrations [Fig. 7(a)]. Upon application of electric field, the perturbation modes grow and a phase difference appears in the spatial distribution of acid and base concentrations. For example, the spatial variation of species concentrations at $t = 150$ s in Fig. 7(a) is similar to the unstable mode depicted in Fig. 6. As explained above, the phase difference in perturbation modes of acid and base cause spatial variations in pH and electromigration flux, which tend to destabilize the electrophoretic system. The phase difference between spatial distribution of acid and base concentrations at later times can be explained by noting that small concentration perturbations can be considered as linear combination of stable and unstable eigenmodes predicted by linear stability analysis [Fig. 7(b)]. Over time, the unstable mode grows while the stable mode diminishes and hence the concentration field predicted by nonlinear simulations at $t = 150$ s in Fig. 7(a) resembles the unstable eigenmode predicted by linear stability analysis [Fig. 7(b)].

We note that the agreement between nonlinear simulations and linearized analysis holds only when concentration disturbances are small compared with base state species concentrations. When the base-state concentrations and disturbances have comparable magnitude nonlinearities due to coupling of local electric field with species concentrations set in. Consequently, the nonlinear electromigration flux leads to distortion of concentration modes disturbances as seen at $t = 500$ s in Fig. 7(a).

IV. CONCLUDING REMARKS

We have performed linear stability analysis to study the cause and nature of instabilities in so-called "oscillating electrolyte" systems. We modeled the growth of concentration disturbances by linearizing the nonlinear species transport

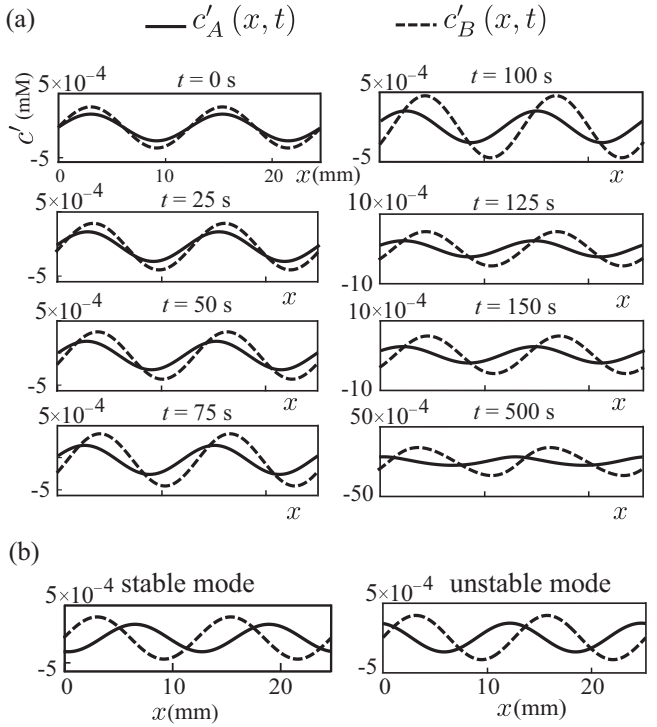

FIG. 7. Growth of concentration disturbances during unstable electrophoretic transport of ions. (a) Nonlinear simulation showing evolution of concentration disturbances during unstable electrophoretic transport. At $t = 0$ s, the base state with uniform acid and base concentrations is perturbed with in-phase disturbances. Over time, the perturbations in species concentrations grow and a phase difference appears between the concentration distributions of acid and base concentrations. When the concentration disturbances grow to magnitudes comparable to that of the base state ($t =$ 500 s), nonlinearities in electromigration flux distort the concentration disturbances. (b) Stable and unstable eigenmodes predicted by linear stability analysis. Since the unstable mode grows and the stable mode diminishes over time, the concentration distribution predicted by the nonlinear simulation at later times ($t = 150$ s) resembles the unstable mode. These calculations are based on base state consisting of 0.21 mM sebacic acid and 0.323 mM imidazole, and current density of 20.37 Am^{-2}.

equations, which take into account the effects of electromigration, diffusion, and acid-base equilibria. The results of linear stability analysis show that for an oscillating electrolyte system, the growth rates and the range of wave numbers of unstable perturbation modes increase with electric field. Moreover, the destabilizing effect of electromigration and the stabilizing effect of diffusion result in a particular perturbation mode with maximum growth rate. We expect that the most unstable mode should be observable during the initial phase of instability when perturbations in concentration field are small. Our analysis also yields the scaling of growth rates and wave number of most unstable mode with electric field. We have verified this scaling using full nonlinear simulations of species transport equations for electrophoresis. We also showed that the oscillating behavior is exhibited only over a certain range of acid and base concentrations.

In addition to linear stability analysis, we have discussed the physical mechanism underlying electrophoretic transport instabilities in certain binary electrolytes. We showed that the unstable behavior is exhibited by binary electrolytes containing multivalent species having unusually high electrophoretic mobilities in higher ionization states. Presence of such multivalent species causes abnormal change in conductivity due to minor disturbances in the concentration field. The abnormal variations in conductivity then alter the local electric field in a way that further destabilizes the electrophoretic transport of ions. We note that oscillating behavior is not observed in a majority of electrophoretic processes. However, in certain electrophoresis experiments local electrolyte composition may be favorable to oscillations leading to spurious gradients in species concentrations.

ACKNOWLEDGMENT

The authors acknowledge the financial support received from the Science and Engineering Research Board (SERB), Government of India under Grant No. SERB/F/2665/2014-2015.

APPENDIX: DERIVATION OF LINEARIZED SPECIES TRANSPORT EQUATIONS

To derive the linearized species transport equations for a binary electrolyte system, we first eliminate the perturbation electric field $\mathbf{E}'$ from Eqs. (19) and (20) using Eq. (21) to get

$$\frac{\partial}{\partial t}\begin{pmatrix} c'_A \\ c'_B \end{pmatrix} + \mathbf{M_1} E_0 \frac{\partial}{\partial x}\begin{pmatrix} c'_{A,0} \\ c'_{A,-1} \\ c'_{A,-2} \\ c'_{B,0} \\ c'_{B,1} \\ \sigma' \\ S' \end{pmatrix} = \mathbf{D_1}\nabla^2 \begin{pmatrix} c'_{A,0} \\ c'_{A,-1} \\ c'_{A,-2} \\ c'_{B,0} \\ c'_{B,1} \\ \sigma' \\ S' \end{pmatrix}, \quad \text{(A1)}$$

where $\mathbf{M_1}$ and $\mathbf{D_1}$ are given by

$$\mathbf{M_1} = \begin{pmatrix} 0 & \mu_{A,-1} & \mu_{A,-2} & 0 & 0 & -\overline{\mu}_A \overline{c_A}/\overline{\sigma} & 0 \\ 0 & 0 & 0 & 0 & \mu_{B,1} & -\overline{\mu}_B \overline{c_B}/\overline{\sigma} & 0, \end{pmatrix}, \quad \text{(A2)}$$

$$\mathbf{D_1} = \begin{pmatrix} D_{A,0} & D_{A,-1} & D_{A,-2} & 0 & 0 & 0 & -\overline{\mu}_A \overline{c_A}/\overline{\sigma} \\ 0 & 0 & 0 & D_{B,0} & D_{B,1} & 0 & -\overline{\mu}_B \overline{c_B}/\overline{\sigma} \end{pmatrix}. \quad \text{(A3)}$$

In order to write Eq. (A1) in terms of total concentrations of acid (c'_A) and base (c'_B), it is necessary to relate $c'_{A,0}, c'_{A,-1}, c'_{A,-2}, c'_{B,1}, c'_{B,0}, \sigma'$, and S' with c'_A and c'_B. Relating the perturbation concentrations of various ionization states of

acid and base with their total concentrations by Eq. (24), we get

$$\mathbf{N_1}\nabla\begin{pmatrix} c'_{A,0} \\ c'_{A,-1} \\ c'_{A,-2} \\ c'_{B,0} \\ c'_{B,1} \\ \sigma' \\ S' \end{pmatrix} = \mathbf{M_2}\nabla\begin{pmatrix} c'_A \\ c'_B \\ c'_H \end{pmatrix}, \tag{A4}$$

$$\mathbf{N_1} = \begin{pmatrix} 1 & 0 & 0 & 0 & 0 & 0 & 0 \\ 0 & 1 & 0 & 0 & 0 & 0 & 0 \\ 0 & 0 & 1 & 0 & 0 & 0 & 0 \\ 0 & 0 & 0 & 1 & 0 & 0 & 0 \\ 0 & 0 & 0 & 0 & 1 & 0 & 0 \\ 0 & \mu_{A,-1}F & 2\mu_{A,-1}F & 0 & -\mu_{B,1}F & 1 & 0 \\ 0 & D_{A,-1}F & 2D_{A,-1}F & 0 & -D_{B,1}F & 0 & 1 \end{pmatrix}, \tag{A5}$$

$$\mathbf{M_2} = \begin{pmatrix} \overline{g}_{A,0} & 0 & \overline{G}_{A,0} \\ \overline{g}_{A,-1} & 0 & \overline{G}_{A,-1} \\ \overline{g}_{A,-2} & 0 & \overline{G}_{A,-2} \\ 0 & \overline{g}_{B,0} & \overline{G}_{B,0} \\ 0 & \overline{g}_{B,1} & \overline{G}_{B,1} \\ 0 & 0 & \left(\mu_H + \mu_{OH}\frac{K_w}{\overline{c}_H^2}\right)F \\ 0 & 0 & \left(D_H + D_{OH}\frac{K_w}{\overline{c}_H^2}\right)F \end{pmatrix}, \tag{A6}$$

where

$$\overline{c}_i \left.\frac{\partial g_{i,z}}{\partial c_H}\right|_{c_H=\overline{c}_H} = \overline{G}_{i,z}. \tag{A7}$$

Next, we relate the perturbation hydronium ion concentration c'_H with c'_A and c'_B, using Eq. (25) to get

$$\begin{pmatrix} c'_A \\ c'_B \\ c'_H \end{pmatrix} = \mathbf{M_3}\begin{pmatrix} c'_A \\ c'_B \end{pmatrix}, \tag{A8}$$

$$\mathbf{M_3} = \begin{pmatrix} 1 & 0 \\ 0 & 1 \\ \frac{\overline{g}_{A,-1}+2\overline{g}_{A,-2}}{P} & -\frac{\overline{g}_{B,1}}{P} \end{pmatrix}, \tag{A9}$$

where P is given by

$$P = \left(1 + \frac{K_w}{\overline{c}_H^2} - \overline{G}_{A,-1} - 2\overline{G}_{A,-2} + \overline{G}_{B,1}\right). \tag{A10}$$

Finally, combining Eqs. (A1)–(A10) we arrive at the linearized governing equations for perturbation concentrations of acid and base,

$$\frac{\partial}{\partial t}\begin{pmatrix} c'_A \\ c'_B \end{pmatrix} + \mathbf{M}E_0\frac{\partial}{\partial x}\begin{pmatrix} c'_A \\ c'_B \end{pmatrix} = \mathbf{D}\nabla^2\begin{pmatrix} c'_A \\ c'_B \end{pmatrix}, \tag{A11}$$

where $\mathbf{M}$ and $\mathbf{D}$ are given by

$$\mathbf{M} = \mathbf{M_1}\mathbf{N_1^{-1}}\mathbf{M_2}\mathbf{M_3} \quad \text{and} \quad \mathbf{D} = \mathbf{D_1}\mathbf{N_1^{-1}}\mathbf{M_2}\mathbf{M_3}. \tag{A12}$$

The matrices $\mathbf{M}$ and $\mathbf{D}$ have units of mobility and diffusivity, respectively.

[1] J. W. Jorgenson and K. D. Lukacs, Science **222**, 266 (1983).
[2] G. Garcia-Schwarz, A. Rogacs, S. S. Bahga, and J. Santiago, J. Vis. Exp. **61**, e3890 (2012).
[3] R. Bharadwaj and J. Santiago, J. Fluid Mech. **543**, 57 (2005).
[4] M. Stedry, M. Jaros, K. Vcelakova, and B. Gas, Electrophoresis **24**, 536 (2003).
[5] S. S. Bahga, M. Bercovici, and J. G. Santiago, Electrophoresis **33**, 3036 (2012).
[6] M. Y. Zhukov, USSR Comput. Math. Math. Phys. **24**, 138 (1984).
[7] V. Hruska, M. Jaros, and B. Gas, Electrophoresis **27**, 513 (2006).
[8] M. Stedry, M. Jaros, V. Hruska, and B. Gas, Electrophoresis **25**, 3071 (2004).
[9] M. Riesová, V. Hruška, E. Kenndler, and B. Gaš, J. Phys. Chem. B **113**, 12439 (2009).
[10] D. Saville and O. Palusinski, AIChE J. **32**, 207 (1986).
[11] S. S. Bahga, M. Bercovici, and J. G. Santiago, Electrophoresis **31**, 910 (2010).